Association of sinking organic matter with various types of mineral ballast in the deep sea: Implications for the rain ratio

Christine Klaas[1] and David E. Archer
Department of the Geophysical Sciences, University of Chicago, Chicago, Illinois, USA

[1]   We compiled and standardized sediment trap data below 1000 m depth from 52 locations around the globe to infer the implications of the *Armstrong et al.* [2002] "ballast" model to the ratio of organic carbon to calcium carbonate in the deep sea (the rain ratio). We distinguished three forms of mineral ballast: calcium carbonate, opal, and lithogenic material. We concur with *Armstrong et al.* [2002] that organic carbon sinking fluxes correlate tightly with mineral fluxes. Based on the correlations seen in the trap data, we conclude that most of the organic carbon rain in the deep sea is carried by calcium carbonate, because it is denser than opal and more abundant than terrigenous material. This analysis explains the constancy of the organic carbon to calcium carbonate rain ratio in the deep sea today, and argues against large changes in the mean value of this ratio in the past. However, sediment trap data show variability in the ratio in areas of high relative calcium carbonate export (mass $CaCO_3$/mass ratio > 0.4), unexplainable by the model, leaving open the possibility of regional variations in the rain ratio in the past.   *INDEX TERMS:* 1615 Global Change: Biogeochemical processes (4805); 1635 Global Change: Oceans (4203); 4863 Oceanography: Biological and Chemical: Sedimentation; *KEYWORDS:* organic carbon flux, sediment traps, marine carbon cycle, oceanography, rain ratio

1.   Introduction

[2]   Model studies have proposed an increase in ocean pH as a mechanism to explain the decrease in atmospheric pCO_2 during glacial time [*Archer et al.*, 2000]. The increase in pH of the ocean could be driven by an increase in the weathering minus shallow water $CaCO_3$ deposition [*Opdyke and Walker*, 1992], but the lysocline signature of an increase in deep sea $CaCO_3$ burial during the last glacial maximum is not seen [*Archer and Maier-Reimer*, 1994; *Catubig et al.*, 1998]. The pH of the ocean may also be sensitive to the ratio of particulate organic carbon (POC) to $CaCO_3$ or particulate inorganic carbon (PIC) raining to the deep sea (the POC/PIC rain ratio), which may have a smaller impact on the distribution of $CaCO_3$ on the seafloor [*Archer et al.*, 2000].

[3]   Export of POC into the deep ocean is thought to be driven primarily by growth and sedimentation of diatoms following nutrient injection events due to winter convection or upwelling [*Peinert et al.*, 1989; *Smetacek et al.*, 1990; *Ittekkot et al.*, 1991; *Honjo*, 1996; *Takahashi et al.*, 2000]. $CaCO_3$ production, mediated primarily by coccoli-

thophores, is thought to increase when diatom growth is limited by availability of silica or iron [*Margalef*, 1978; *Tyrell and Taylor*, 1996]. However, if organic carbon export to the deep sea were associated primarily with diatom production at the sea surface, we would expect regional variability in the rain ratio that is not observed in trap data, and could not be tolerated by models of $CaCO_3$ preservation on the seafloor [*Archer*, 1996]. *Armstrong et al.* [2002] and *François et al.* [2002] propose that organic carbon export is determined by the presence of ballast minerals (opal, calcium carbonate and lithogenic material). The model of *Armstrong et al.* [2002] partitions POC in sinking matter into two fractions: a ballast-associated fraction with remineralization scale similar to the dissolution scales of the minerals, and a "free" POC fraction which decays in the top kilometer or so. Either the ballast increases the sinking speed of the organic matter, as implied by the term ballast, or it could provide some physical protection from degradation through adsorption or other interaction between organic matter and minerals. *Armstrong et al.* [2002] found significant geographical differences in the POC fraction associated with the mineral fraction and hypothesized that such differences might be related to differences in composition of the ballast material. The purpose of this study is to synthesize a global long-term sediment trap data set to investigate the relationship between mineral fractions (opal, calcium carbonate

---

[1]Now at Max-Planck-Institute for Biogeochemistry, Jena, Germany.

and lithogenic material) and the transfer of POC to the deep ocean, based on the model of *Armstrong et al.* [2002].

2. Methods

2.1. Data

[4] We compiled time series and composite annual flux data from sediment trap experiments at 52 different locations with a minimum duration of 10 months and at depths ranging from 1000 to 4833 m (Figure 1, Table 1).

[5] Biogenic silica fluxes were determined using different methods depending on authors. The most widespread methods are modifications of the sodium carbonate/sodium hydroxide sequential leaching method. Some authors, however, use a normative method based on aluminum and total silica (biogenic and lithogenic) measurements and assuming a Si/Al ratio varying from 3 to 3.5 for lithogenic component of the silica fluxes. In this study we standardized estimates on an Al/Si ratio of 3 when no biogenic silica determination was carried out. Directly measured biogenic silica fluxes were corrected by standardizing the water fraction using a water/silicon weight ratio of 0.256 (10% water, [*Mortlock and Froelich*, 1989]). For trap experiments where only the combustible fraction was measured, POC has been estimated using a particulate organic matter (POM) to POC ratio of 2.199 (Figure 2). This ratio was obtained though regression analysis of POC versus POM from trap experiments in the San Pedro Basin [*Thunell et al.*, 1994] and from suspended matter analysis in the Southern Ocean [*Suess and Ungerer*, 1981]. POM values were estimated from the measured combustible fraction corrected in both data sets for water content of opal [*Tsunogai and Noriki*, 1987] using a water/silicon weight ratio of 0.256 [*Mortlock and Froelich*, 1989]. The lithogenic component in the traps was estimated as total mass less calcium carbonate ($CaCO_3$), opal ($SiO_2 0.4 H_2O$), and organic matter (POC*2.199 or the combustible fraction less water content of measured opal flux). For a few trap experiments, data on the fraction of POC and opal that was remineralized or dissolved in the cups was available [*Honjo and Manganini*, 1993; *Honjo et al.*, 1995] and was added to the particulate fluxes.

[6] Errors for the annual flux data compiled in this study were estimated whenever analytical errors were given by the authors. Splitting errors were accounted for using the given values, or assumed to be 6%, the maximum value found in the literature [*von Bodungen*, 1991; *Honjo and Manganini*, 1993; *Honjo et al.*, 1995, 1999, 2000; *Nodder and Northcote*, 2001]. A few studies give estimates of the fraction of material dissolved or remineralized in the sampling cups (POC and/or silica) together with analytical errors. In such cases analytical error of the dissolved fraction was included in the error calculations. Error estimates could be obtained for traps at 21 different locations (Table 1).

2.2. Mineral-Associated POC Flux Model

[7] The formulation of *Armstrong et al.* [2002] is a mechanistic model that was developed as a best fit to the vertical variations in POC with depth as measured in sediment traps. The model assumes that part of the export POC is associated with a ballast fraction and is proportional to this fraction. The excess POC is considered the free fraction:

$$F_p = F_e + f.F_b, \tag{1}$$

where F_p is the total export POC mass flux, F_e is the mass flux of the free POC, F_b is the total ballast mass flux, and f is a proportionality factor, essentially the POC carrying capacity or coefficient of the ballast. The different components of the POC sinking flux decrease with depth according to exponential or power law functions

$$F(z) = F_e.f(z, \partial_e) + f.F_b.f(z, \partial_b), \tag{2}$$

where F(z) is the total POC flux at depth z, f(z, ∂_e) and f(z, ∂_b) are decay functions for free and ballasted POC.
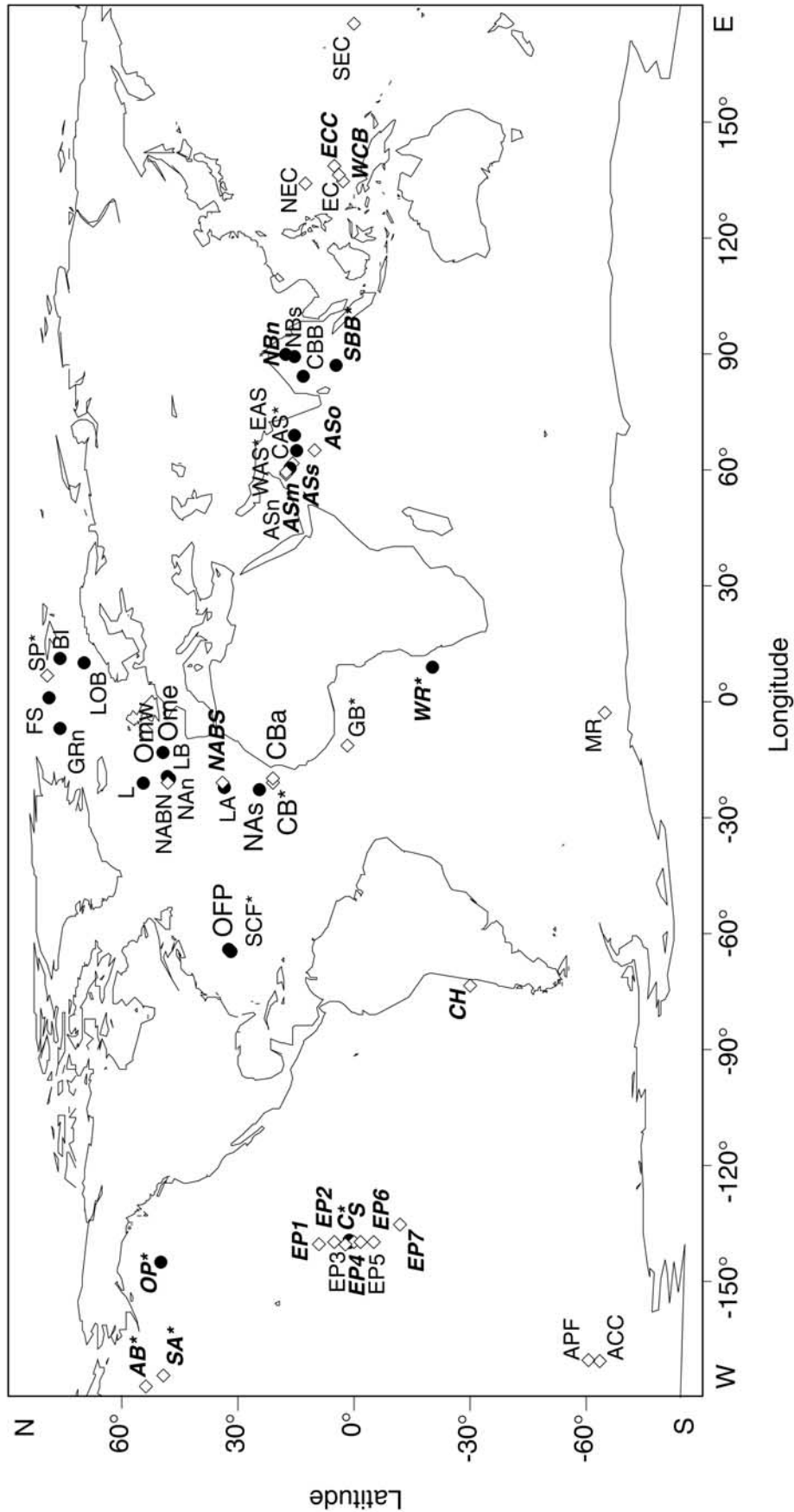
[8] Here we extend the application of the model by distinguishing the different forms of mineral ballast ($CaCO_3$, opal (SiO_2 0.4 H_2O), and lithogenic terrigenous material (clays)) to predict large scale variability of the POC/PIC rain ratio in the deep sea as suggested by *Armstrong et al.* [2002]. Based on the approximately 500 meter depth decay scale for "free" POC from *Armstrong et al.* [2002], we first assume that below 1000 m the free POC flux is negligible. The model reduces to:

$$F(z) = f_{ca}.F_{ca}(z) + f_o.F_o(z) + f_l.F_l(z), \tag{3}$$

where $F_o(z)$, $F_{ca}(z)$, and $F_l(z)$ are the mass fluxes of $CaCO_3$, opal, and lithogenic material at depth z. The carrying coefficients f can be determined by multiple linear regression of trap data below 1000 m depth.

3. Results

[9] Scatterplots of POC versus mineral constituents of annual fluxes for trap experiments below 1000 m depth are given in Figure 3 and indicate a tendency toward increasing POC with mineral flux ($CaCO_3$, opal, and lithogenic material). Multiple correlation analysis of POC fluxes as a function of mineral fraction (in mass units) for different trap data sets is highly significant with a correlation coefficient varying from 0.956–0.985 (Table 2). The carrying coefficients are highest for $CaCO_3$ and lowest for opal mass fluxes. Using different data sets for the analysis does not change significantly carrying coefficients for the different mineral fractions, however, the carrying coefficients tend to decrease when using deep trap data, suggesting that a small fraction of the POC transported to 1000 m is remineralized before reaching the sediments. Overall carrying coefficients determined using trap experiments below 2000 m seem to show the least uncertainty. If the data set is reduced to sediment trap experiments carried out in open ocean areas far from influence of "exogenous" sources such as resuspended sediments from continental shelves or ice-rafted debris ("selected" sediment trap experiments, Figure 1), the coefficients for $CaCO_3$ and opal do not change much. The coefficient for the lithogenic fraction shows the highest

Figure 1. Location and code names of trap experiments compiled in this study. Solid circles indicate locations where only annual flux values were available. Open diamonds indicate locations where both annual and individual cup data could be obtained. Trap names with asterisks correspond to experiments covering 2 years or longer. Trap names in bold italic characters correspond to the "selected" trap experiments with little influence from "exogenous" material such as ice-rafted debris or resuspended sediments.

Table 1. Location, Water Depth, Trap Depth, Period Sampled, Duration, Codes and References of the Annual Trap Experiment Data Used in This Study
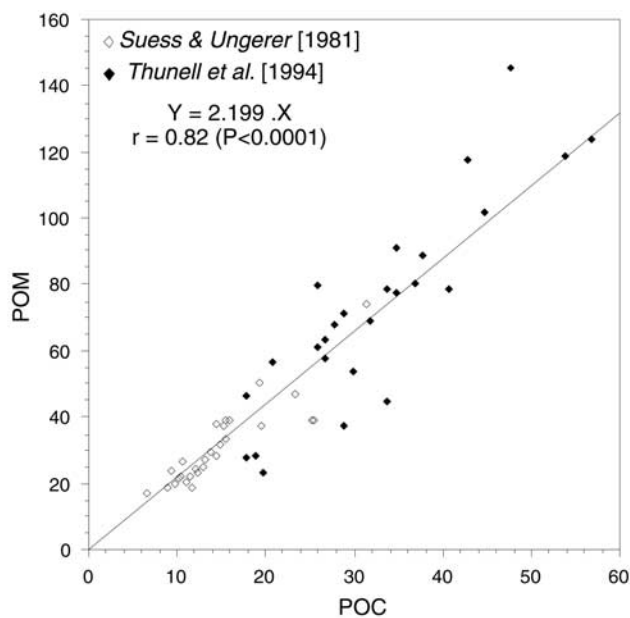
Latitude	Longitude	Water Depth, m	Trap Depth, m	Sampling Period	Duration, days	Code	Reference
53°32.0′N	176°56.2′W	3783	3193	7/8/90 – 17/7/91	344	AB1	*Takahashi et al.* [2000]
53°31.0′N	177°05.0′W	3790	3200	7/8/91 – 31/7/92	359	AB2	*Takahashi et al.* [2000]
53°29.9′N	177°04.2′W	3789	3199	2/8/93 – 7/6/94	309	AB4	*Takahashi et al.* [2000]
53°30.4′N	176°59.7′W	3788	3198	4/8/94 – 25/7/95	355	AB5	*Takahashi et al.* [2000]
63°09.0′S	169°54.0′W	2885	1031	1/1/97 – 27/1/98	425	ACC[a]	*Honjo et al.* [2000]
60°17.0′S	170°03.0′W	3957	1003	1/1/97 – 27/1/98	425	APF[a]	*Honjo et al.* [2000]
17°12.0′N-	59°36.0′E-	3465-	1857-	11/11/94 – 24/12/95	391	ASm[a]	*Honjo et al.* [1999]
17°13.0′N	59°36.0′E	3477	1882	–·–		"	*Honjo et al.* [1999]
17°12.0′N-	59°36.0′E-	3465-	2871-	11/11/94 – 24/12/95	391	ASm[a]	*Honjo et al.* [1999]
17°13.0′N	59°36.0′E	3447	2991	–·–		"	*Honjo et al.* [1999]
17°24.0′N	58°48.0′E-	3642-	3141-	11/11/94 – 24/12/95	391	ASn[a]	*Honjo et al.* [1999]
"	58°48.0′E	3655	3159	–·–		"	*Honjo et al.* [1999]
10°00.0′N	65°00.0′E	4411	2363	28/11/94 – 24/12/95	391	ASo[a]	*Honjo et al.* [1999]
10°00.0′N	65°00.0′E	4411	3915	28/11/94 – 24/12/95	391	ASo[a]	*Honjo et al.* [1999]
15°20.0′N-	61°30.0′E	3974-	2229-	11/11/94 – 7/12/95	374	ASs[a]	*Honjo et al.* [1999]
12°59.0′N	61°30.0′E	3983	2215	–·–		"	*Honjo et al.* [1999]
15°20.0′N-	61°30.0′E-	3974-	3478-	11/11/94 – 24/12/95	391	ASs[a]	*Honjo et al.* [1999]
12°59.0′N	61°30.0′E	3983	3489	–·–		"	*Honjo et al.* [1999]
75°51.0′N	11°28.0′E	2123	1650	12/07/84 – 10/07/85	363	BI	*Honjo et al.* [1988]
1°00.0′N	139°00.0′W	4470	1095	12/12/82 – 25/2/84	428	C3	*Dymond and Collier* [1988]
1°00.0′N	139°00.0′W	4470	1895	12/12/82 – 25/2/84	428	C3	*Dymond and Collier* [1988]
1°00.0′N	139°00.0′W	4470	3495	12/12/82 – 25/2/84	428	C3	*Dymond and Collier* [1988]
1°00.0′N	139°00.0′W	4470	1083	25/2/84 – 22/2/85	363	C4	*Dymond and Collier* [1988]
1°00.0′N	139°00.0′W	4470	1883	25/2/84 – 22/2/85	363	C4	*Dymond and Collier* [1988]
1°00.0′N	139°00.0′W	4470	2908	25/2/84 – 22/2/85	363	C4	*Dymond and Collier* [1988]
14°29.0′N-	64°46.0′E-	3912-	2894-	20/11/86 – 2/5/87	>305	CAS1[a]	*Haake et al.* [1993]; *Ramaswamy and Nair* [1994]
14°28.0′N-	64°46.0′E-	3890-	2913-	12/5/87 – 21/10/87		"	*Haake et al.* [1993]; *Ramaswamy and Nair* [1994]
14°33.0′N	64°47.0′E	3910	2933	22/11/87 – 31/10/88		"	*Haake et al.* [1993]; *Ramaswamy and Nair* [1994]
14°33.0′N-	64°47.0′E	3910-	2933-	22/11/87 – 31/10/88	>305	CAS2[a]	*Haake et al.* [1993]; *Ramaswamy and Nair* [1994]
14°36.0′N	"	3906	3109	20/11/88 – 24/2/89		"	*Haake et al.* [1993]; *Ramaswamy and Nair* [1994]
21°08.7′N	20°41.2′W	4092	3502	15/3/89 – 24/3/90	374	CB1[a]	*Wefer and Fischer* [1993]
21°08.0′N-	20°40.0′W	4094-	3557-	1/1/91 – 19/11/91	298	CB2[a]	*Fischer and Wefer* [1996]
21°09.0′N	20°41.0′W	4108	3562	–·–		"	*Fischer and Wefer* [1996]
20°55.3′N	19°44.5′W	3646	2195	22/3/88 – 8/3/89	351	CBa[a]	*Wefer and Fischer* [1993]
13°09.0′N-	84°22.0′E-	3259-	2282-	28/10/87 – 28/2/88	312	CBB1	*Ittekkot et al.* [1991]; *Schäfer et al.* [1996]
"	84°21.0′E	3263	2227	4/1/88 – 10/6/88		"	*Ittekkot et al.* [1991]; *Schäfer et al.* [1996]
13°09.0′N	84°21.0′E	3263	2286	2/11/88 – 19/10/89	351	CBB2	*Ittekkot et al.* [1991]; *Schäfer et al.* [1996]
13°09.0′N	84°20.0′E	3267	2282	5/12/90 – 26/10/91	325	CBB3	*Ittekkot et al.* [1991]; *Schäfer et al.* [1996]
30°01.1′S-	73°11.0′W-	4360	2323	22/07/93 – 26/6/94	340	CH	*Hebbeln et al.* [2000]
30°00.3′S	73°10.3′W	4360	2323	–·–		"	*Hebbeln et al.* [2000]
15°28.0′N-	68°45.0′E-	3782-	2764-	20/11/86 – 2/5/87	>305	EAS[a]	*Haake et al.* [1993]; *Ramaswamy and Nair* [1994]
15°26.0′N-	68°43.0′E-	3770-	2763-	12/5/87 – 21/10/87		"	*Haake et al.* [1993]; *Ramaswamy and Nair* [1994]
15°32.0′N	68°45.0′E-	3782	2778	22/11/87 – 31/10/88		"	*Haake et al.* [1993]; *Ramaswamy and Nair* [1994]
4°07.5′N	136°16.6′E	4888	1769	4/6/91 – 15/4/92	317	EC[a]	*Kawahata et al.* [2000]
4°07.5′N	136°16.6′E	4888	4574	4/6/91 – 15/4/92	317	EC[a]	*Kawahata et al.* [2000]
5°00.6′N	138°49.8′E	4130	1130	21/11/88 – 16/12/89	390	ECC	*Kempe and Knaack* [1996]
5°00.6′N	138°49.8′E	4130	3130	21/11/88 – 16/12/89	390	ECC	*Kempe and Knaack* [1996]
9°00.0′N	139°59.0′W	5100	2150	2/2/92 – 7/1/93	357	EP1[a]	*Honjo et al.* [1995]
9°00.0′N	139°59.0′W	5100	2250	2/2/92 – 7/1/93	357	EP1[a]	*Honjo et al.* [1995]
5°01.0′N	139°47.0′W	4493	1191	2/2/92 – 7/1/93	357	EP2[a]	*Honjo et al.* [1995]
5°01.0′N	139°47.0′W	4493	2091	2/2/92 – 7/1/93	357	EP2[a]	*Honjo et al.* [1995]
5°01.0′N	139°47.0′W	4493	3793	2/2/92 – 7/1/93	357	EP2[a]	*Honjo et al.* [1995]
2°00.0′N	140°08.0′W	4397	2203	2/2/92 – 7/1/93	357	EP3[a]	*Honjo et al.* [1995]
0°04.0′N	139°45.0′W	4358	2284	2/2/92 – 7/1/93	357	EP4[a]	*Honjo et al.* [1995]
0°04.0′N	139°45.0′W	4358	3618	2/2/92 – 7/1/93	357	EP4[a]	*Honjo et al.* [1995]
1°57.0′S	139°45.0′W	4293	3593	2/2/92 – 7/1/93	357	EP5[a]	*Honjo et al.* [1995]
4°57.0′S	139°44.0′W	4198	2099	2/2/92 – 7/1/93	357	EP6[a]	*Honjo et al.* [1995]
4°57.0′S	139°44.0′W	4198	2209	2/2/92 – 7/1/93	357	EP6[a]	*Honjo et al.* [1995]
4°57.0′S	139°44.0′W	4198	2316	2/2/92 – 7/1/93	357	EP6[a]	*Honjo et al.* [1995]
11°58.0′S	135°02.0′W	4294	1292	2/2/92 – 7/1/93	357	EP7[a]	*Honjo et al.* [1995]
11°58.0′S	135°02.0′W	4294	3594	2/2/92 – 7/1/93	357	EP7[a]	*Honjo et al.* [1995]
78°52.0′N	1°22.0′E	ng	2440	20/8/84 – 15/8/85	360	FS	*Honjo* [1990]
1°47.5′N	11°07.6′W	4481	3921	1/3/89 – 25/2/90	361	GB1[a]	*Wefer and Fischer* [1993]
1°48.0′N	11°08.0′W	4481-	3921-	1/1/90 – 31/12/90	327	GB2[a]	*Fischer and Wefer* [1996]
1°47.0′N	"	4522	3965	–·–		"	*Fischer and Wefer* [1996]
75°35.0′N	6°43.0′W	ng	2871	4/8/85 – 3/8/86	364	GRn	*Honjo* [1990]
54°32.0′N	21°04.0′W	2979	2200	10/6/92 – 12/5/93	336	L1	*Kuss and Kremling* [1999]

Table 1. (continued)

Latitude	Longitude	Water Depth, m	Trap Depth, m	Sampling Period	Duration, days	Code	Reference
54°32.0′N	21°04.0′W	2979	2880	10/6/92–12/5/93	336	L1	*Kuss and Kremling* [1999]
33°09.0′N	21°59.0′W	5303	4000	20/9/93–1/9/94	346	LA	*Kuss and Kremling* [1999]
47°48.0′N	19°47.0′W	4574	1030	10/6/92–26/5/93	351	LB1	*Kuss and Kremling* [1999]
47°48.0′N	19°47.0′W	4574	2030	10/6/92–26/5/93	351	LB1	*Kuss and Kremling* [1999]
47°48.0′N	19°47.0′W	4574	3530	10/6/92–26/5/93	351	LB1	*Kuss and Kremling* [1999]
69°30.0′N	10°00.0′E	ng	2760	ng	>305	LOB	*Honjo* [1990]
64°55.0′S	2°30.0′W	5000	4456	20/1/87–20/11/87	304	MR	*Wefer et al.* [1990]
47°42.9′N-	20°52.5′W-	4418-	1018-	3/4/89–26/9/89	358	NABN	*Honjo and Manganini* [1993]
47°43.6′N	20°51.5′W	4451	1202	16/10/89–16/4/90		"	*Honjo and Manganini* [1993]
47°42.9′N-	20°52.5′W-	4418-	3718-	3/4/89–26/9/89	358	NABN	*Honjo and Manganini* [1993]
47°43.6′N	20°51.5′W	4451	3749	16/10/89–16/4/90		"	*Honjo and Manganini* [1993]
33°49.3′N-	21°00.5′W-	5261-	2067-	3/4/89–26/9/89	358	NABS	*Honjo and Manganini* [1993]
33°48.4′N	21°02.2′W	5083	1894	16/10/89–16/4/90		"	*Honjo and Manganini* [1993]
33°49.3′N-	21°00.5′W-	5261-	4564-	3/4/89–26/9/89	358	NABS	*Honjo and Manganini* [1993]
33°48.4′N	21°02.2′W	5083	4391	16/10/89–16/4/90		"	*Honjo and Manganini* [1993]
47°50.0′N	19°30.0′W	4440	3100	18/4/89–17/9/90	502	NAn	*Jickells et al.* [1996]
24°33.0′N	22°50.0′W	4860	3870	14/10/90–27/9/91	348	NAs	*Jickells et al.* [1996]
17°26.0′N-	89°35.0′E-	2263-	1727-	28/10/87–28/2/88	312	NBn	*Ittekkot et al.* [1991]; *Schäfer et al.* [1996]
17°27.0′N	89°36.0′E	2267	1790	1/4/88–6/10/88		"	*Ittekkot et al.* [1991]; *Schäfer et al.* [1996]
17°27.0′N	89°36.0′E	2265	2029	2/11/88–19/10/89	351	NBn	*Ittekkot et al.* [1991]; *Schäfer et al.* [1996]
15°31.0′N	89°13.0′E	2706	2120	5/12/90–26/10/91	325	NBs	*Ittekkot et al.* [1991]; *Schäfer et al.* [1996]
12°01.0′N	134°17.2′E	5300	4300	21/11/88–16/12/89	390	NEC	*Kempe and Knaack* [1996]
31°50.0′N	64°30.0′W	±4500	3200	14/1/88–30/1/89	372	OFP4	*Conte et al.* [2001]
49°11.2′N	12°49.2′W	ng	1050	1/07/93–3/9/94	368	Ome	*Wollast and Chou* [1998]; *Antia et al* [1999]
49°05.0′N	13°25.8′W	ng	1440	1/07/93–3/9/94	368	Omw	*Wollast and Chou* [1998]; *Antia et al* [1999]
49°05.0′N	13°25.8′W	ng	3260	1/07/93–3/9/94	368	Omw	*Wollast and Chou* [1998]; *Antia et al* [1999]
50°00.0′N	145°00.0′W	4240	3800	23/9/82–23/4/84	365	OP1	*Wong et. al.* [1999]
50°00.0′N	145°00.0′W	4240	1000	20/11/84–23/4/86	360	OP3	*Wong et. al.* [1999]
50°00.0′N	145°00.0′W	4240	3800	20/11/84–23/4/86	>360	OP3	*Wong et. al.* [1999]
50°00.0′N	145°00.0′W	4240	3800	19/10/86–6/5/88	365	OP4	*Wong et. al.* [1999]
50°00.0′N	145°00.0′W	4240	3800	11/12/88–2/5/90	365	OP6	*Wong et. al.* [1999]
50°00.0′N	145°00.0′W	4240	1000	13/10/89–11/11/90	>360	OP7	*Wong et. al.* [1999]
50°00.0′N	145°00.0′W	4240	3800	13/10/89–11/11/90	>360	OP7	*Wong et. al.* [1999]
50°00.0′N	145°00.0′W	4240	3800	26/9/92–16/5/94	365	OP8	*Wong et. al.* [1999]
11°00.0′N	140°00.0′W	4260	1600	29/12/82–14/2/84	412	S	*Dymond and Collier* [1988]
11°00.0′N	140°00.0′W	4260	3400	29/12/82–14/2/84	412	S	*Dymond and Collier* [1988]
48°59.8′N	173°54.8′W	5400	4806	11/8/91–27/6/92	321	SA2	*Takahashi et al.* [2000]
48°59.5′N	173°58.5′W	5427	4833	10/8/92–27/6/93	321	SA3	*Takahashi et al.* [2000]
49°00.9′N	174°00.0′W	5368	4774	6/8/94–2/8/95	361	SA5	*Takahashi et al.* [2000]
4°28.0′N-	87°19.0′E-	4017-	1040-	28/10/87–28/2/88	312	SBB1	*Ittekkot et al.* [1991]; *Schäfer et al.* [1996]
"	87°18.0′E	4045	1017	1/4/88–6/10/88		"	*Ittekkot et al.* [1991]; *Schäfer et al.* [1996]
4°28.0′N-	87°19.0′E-	4017-	3006-	28/10/87–28/2/88	312	SBB1	*Ittekkot et al.* [1991]; *Schäfer et al.* [1996]
"	87°18.0′E	4045	2983	1/4/88–6/10/88		"	*Ittekkot et al.* [1991]; *Schäfer et al.* [1996]
5°01.0′N	87°09.0′E	3996	3010	5/12/90–26/10/91	325	SBB2	*Ittekkot et al.* [1991]; *Schäfer et al.* [1996]
32°05.0′N	64°15.0′W	4200	3200	7/2/80–10/12/80	293	SCF1	*Deuser et al.* [1981]; *Conte et al.* [2001]
32°05.0′N	64°15.0′W	4200	3200	6/2/81–3/2/82	358	SCF2	*Deuser et al.* [1981]; *Conte et al.* [2001]
32°05.0′N	64°15.0′W	4200	3200	18/1/83–17/2/84	364	SCF3	*Deuser et al.* [1981]; *Conte et al.* [2001]
0°00.2′N	175°09.7′E	4880	4363	1/6/92–16/4/93	319	SEC[a]	*Kawahata et al.* [2000]
78°53.4′N	6°44.5′E	1661	1110	01/07/88–04/06/89	338.5	SP2	*Hebbeln* [2000]
78°52.6′N	6°40.5′E	1676	1125	05/06/89–05/6/90	396	SP3	*Hebbeln* [2000]
16°18.0′N-	60°28.0′E	4018-	3021-	20/11/86–2/5/87	>305	WAS1[a]	*Haake et al.* [1993]; *Ramaswamy and Nair* [1994]
16°19.0′N-	"	4010-	3033-	12/5/87–21/10/87		"	*Haake et al.* [1993]; *Ramaswamy and Nair* [1994]
16°35.0′N	"	4016	3039	22/11/87–31/10/88		"	*Haake et al.* [1993]; *Ramaswamy and Nair* [1994]
16°35.0′N-	60°28.0′E-	4016	3039-	22/11/87–31/10/88	>305	WAS2[a]	*Haake et al.* [1993]; *Ramaswamy and Nair* [1994]
16°24.0′N	60°29.0′E	"	3029	20/11/88–24/2/89		"	*Haake et al.* [1993]; *Ramaswamy and Nair* [1994]
16°19.0′N	60°31.0′E	4013	3016	15/1/90–15/10/90	>305	WAS3[a]	*Haake et al.* [1993]; *Ramaswamy and Nair* [1994]
2°59.8′N	135°1.5′E	4414	1592	4/6/91–15/4/92	317	WCB[a]	*Kawahata et al.* [1998]
2°59.8′N	135°1.5′E	4414	3902	4/6/91–15/4/92	317	WCB[a]	*Kawahata et al.* [1998]
20°04.2′S	9°10.0′E	2217	1640	4/3/88–16/3/89	376	WR1[a]	*Wefer and Fischer* [1993]
20°02.8′S	9°09.3′E	2196	1648	18/3/89–13/3/90	405	WR2[a]	*Wefer and Fischer* [1993]
20°03.0′S-	9°09.0′E-	2208-	1648	1/1/90–31/12/90	353	WR3[a]	*Fischer and Wefer* [1996]
20°02.0′S	9°10.0′E	2263	1648	–·–		"	*Fischer and Wefer* [1996]
20°02.0′S-	9°10.0′E-	2208-	1648-	1/1/91–17/12/91	339	WR4[a]	*Fischer and Wefer* [1996]
20°08.0′S	8°58.0′E	2263	1717	–·–		"	*Fischer and Wefer* [1996]

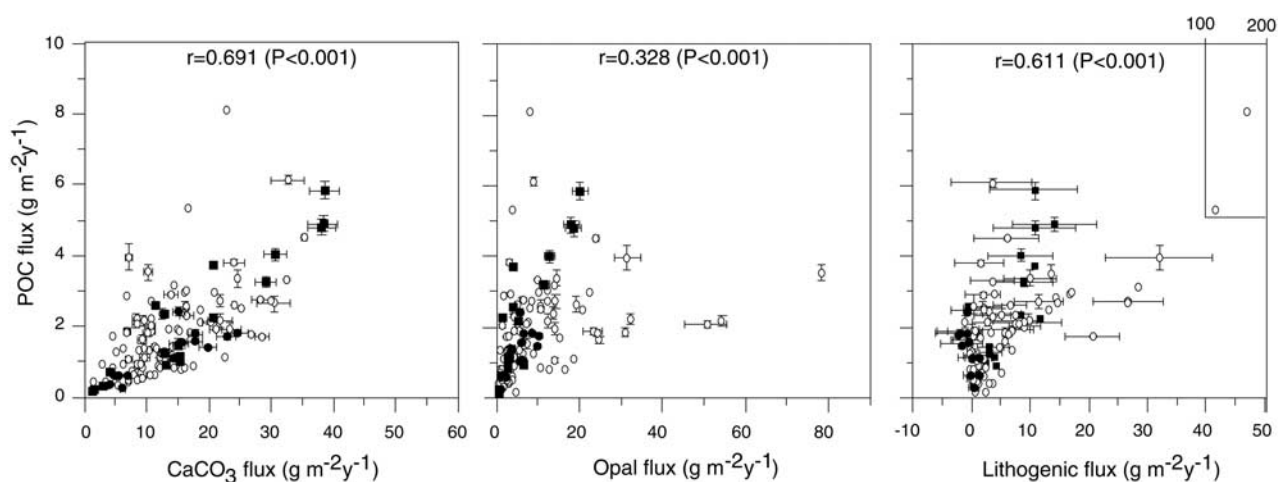[a] Trap experiments for which errors could be estimated.

Figure 2. Regression analysis between Particulate Organic Carbon (POC) and Particulate Organic Matter (POM) estimated from the combustible fraction and opal. Solid diamonds indicate sediment trap experiments. Open diamonds indicate water column data. The regression equation, correlation coefficient and probability are also given in the plot.

variability between data sets and the highest uncertainties (Table 2). These results could indicate that the fraction of carbon associated with the lithogenic fraction is sensitive to the sources and possibly mineralogy of lithogenic particles.

The analysis results for the selected trap data set shows the least variability in the carrying coefficients for lithogenic material and, therefore, seem to give the best results for open ocean conditions. In view of these results following analysis will, therefore, be limited to the selected trap data set.

[10] Carrying coefficients obtained using multiple linear correlation analysis are all significant. However, we find that a single-ballast model (following *Armstrong et al.* [2002]) is almost as good at predicting the overall variability of POC fluxes as the three-ballast model presented above (Table 3). These results seem to contradict the hypothesis that regional difference in POC flux and POC/ PIC rain ratios could be determined by changes in ballast composition. However, comparison of measured versus predicted values (Figure 4) indicates that the three-ballast model is better for predicting POC/PIC rain ratios. Consequently, the single ballast model overestimates POC fluxes in regions where opal dominates ballast fluxes such as the Bering Sea, the Subarctic Pacific and the Southern Ocean and underestimates POC fluxes in areas where $CaCO_3$ and lithogenic material dominate mineral fluxes. None of the models are very good at reproducing geographical variability of PIC/POC rain ratios in areas of intermediate to high $CaCO_3$ versus opal and lithogenic material export fluxes (mass $CaCO_3$/total mass > 0.4, Figure 5), although the three-ballast model gives a better estimate of average values for both POC fluxes and POC/PIC rain ratios (Figure 5, Table 4).
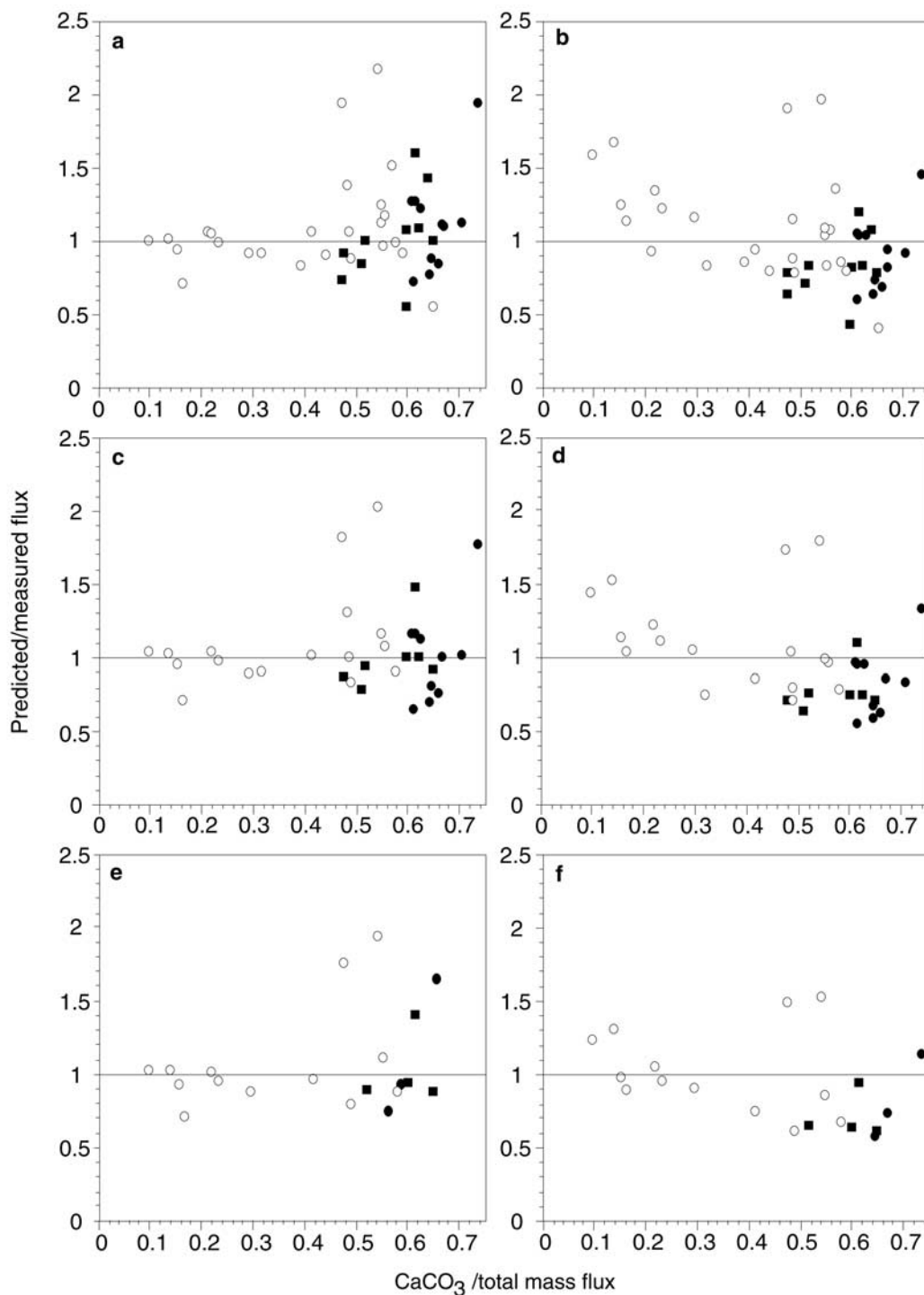
[11] To investigate the causes for the additional regional variability of POC fluxes and POC/PIC rain ratios in areas of high relative $CaCO_3$ fluxes, we tested the possibility that the "free" POC fraction might still be a significant component of the fluxes. These tests assumed the presence of free POC, representing most of the export production near the surface, proportional to surface estimates of primary pro-

Figure 3. Scatterplots, correlation coefficient and probability of particulate organic carbon (POC) flux *versus* $CaCO_3$, opal and lithogenic material fluxes for annual trap experiments. Solid circles indicate trap experiments were the POC and opal fraction remineralized/dissolved in cups was added to the fluxes. Solid squares indicate trap experiments were the opal fraction dissolved in cups was added to the fluxes. Open circles indicate trap experiments not corrected for the particulate fraction remineralized/dissolved in the sampling cups. Error bars correspond to one standard deviation.

Figure 4. (a–f) Scatterplots of the measured versus predicted POC flux, and (g–l) measured versus predicted POC to $CaCO_3$ (as POC/PIC) rain ratio. Values were calculated for models considering 3 mineral fractions (Figures 4a–4c and 4g–4i) or considering only one mineral fraction (sum of total minerals) (Figures 4d–4f and 4j–4l) and using the selected trap experiments carried out below 1000 m depth (Figures 4a, 4d, 4g, and 4j), below 2000 m depth (Figures 4b, 4e, 4h, and 4k) and below 3000 m depth (Figures 4c, 4f, 4i, and 4l). Regression line (solid) and 1:1 line (dashed) between measured and predicted values is given. Solid circles indicate trap experiments were the POC and opal fraction remineralized/dissolved in cups was added to the fluxes. Solid squares indicate trap experiments were the opal fraction dissolved in cups was added to the fluxes. Open circles indicate trap experiments not corrected for the particulate fraction remineralized/dissolved in the sampling cups. Error bars correspond to 1 standard deviation.

Figure 5. Scatterplots of the ratio between predicted and measured values versus mass $CaCO_3$/total mass ratio. Values are presented for models considering (a, c, e) three mineral fractions or considering (b, d, f) only one mineral fraction (sum of total minerals) and using the selected trap experiments carried out below 1000 m depth (Figures 5a and 5b), below 2000 m depth (Figures 5c and 5d) and below 3000 m depth (Figures 5e and 5f). The 1:1 line for the ratio between measured and predicted values is given. Solid circles indicate trap experiments were the POC and opal fraction remineralized/dissolved in cups was added to the fluxes. Solid squares indicate trap experiments were the opal fraction dissolved in cups was added to the fluxes. Open circles indicate trap experiments not corrected for the particulate fraction remineralized/dissolved in the sampling cups.

Table 2. Carrying and Correlation Coefficients for Multiple Correlation Analysis of POC Fluxes Versus Mineral Fluxes[a]

	CaCO3	Opal	Lithogenic	r	N
All traps < 1000 m	0.094 ± 0.010	0.025 ± 0.011	0.035 ± 0.006	0.962	107
Traps-SP < 1000 m	0.090 ± 0.010	0.023 ± 0.011	0.052 ± 0.022	0.956	105
Traps < 2000 m	0.075 ± 0.011	0.029 ± 0.009	0.052 ± 0.018	0.973	78
Traps < 3000 m	0.077 ± 0.012	0.030 ± 0.010	0.039 ± 0.035	0.970	50
Selected < 1000 m	0.083 ± 0.011	0.023 ± 0.010	0.068 ± 0.028	0.976	46
Selected < 2000 m	0.074 ± 0.010	0.025 ± 0.008	0.071 ± 0.030	0.985	34
Selected < 3000 m	0.070 ± 0.025	0.026 ± 0.009	0.065 ± 0.048	0.985	20

[a] Results are given for models separating the mineral fractions in CaCO$_3$, opal and lithogenic material and using trap experiments carried out below 1000 m (<1000 m), below 2000 m (<2000 m) and below 3000 m (<3000 m). All traps (all trap experiments compiled), traps-SP (all traps save SP*). Selected: traps with little or no influence of exogenous material; r: correlation coefficient; N: number of experiments used for the analysis. All correlations coefficients between measured and predicted values are significant (P< 0.0001). SP* traps were separated in the analysis because of the high contribution of ice-rafted debris [*Hebbeln*, 2000]. Errors correspond to the 95% confidence interval of the coefficients.

ductivity (PP) [*Antia et al.*, 2001]. Primary productivity was derived from estimates by *Antoine et al.* [1996] and *Behrenfeld and Falkowski* [1997]. The decay scale for free POC was adopted from *Armstrong et al.* [2002] (e-folding scale of 560 m):

$$F(z) = f_o.F_o(z) + f_{ca}.F_{ca}(z) + f_1.F_1(z) + \beta.PP.e^{(\Delta z/\partial e)} \quad (4)$$

alternatively,

$$F(z) = f_o.F_o(z)f_{ca}.F_{ca}(z) + f_1.F_1(z) + \beta.PP/z \quad (5)$$

As for the carrying coefficients, the proportionality factor (β) determining free POC from primary productivity data can be solved through multiple regression analysis.

[12] Multiple correlation analysis of the selected trap data set indicates that the primary productivity term was not significant for trap experiments below 2000 m depth. When analyzing the selected data set with trap experiments below 1000 m depth, the free POC coefficient is significant only for the model assuming an inverse relationship between free POC and depth ($\beta.PP/z$). The improved model explains at most 22% of POC/PIC rain ratio variability for traps with high mass CaCO$_3$/total mass ratios (still not very good). This corresponds to an total increase from 80 to 84% of the total variance in POC/PIC rain ratios explained for trap experiments below 1000 m depth, not better than results obtained using trap experiment below 2000 m and 3000 m depth (Table 3). In short, including a free POC fraction in the analysis reduces differences between results using data collected at different depth intervals, rather than improving significantly the predictions for POC/PIC rain ratios at high mass CaCO$_3$/total mass ratios. The same tests were done using only trap data with mass CaCO$_3$/total mass >0.4, based on the assumption that in systems with high mass CaCO$_3$/total mass export flux the carrying coefficients for the different mineral fractions might differ. The results are similar to the previous analysis: variability in POC/PIC rain ratios cannot be explained by the three fractions ballast model independent of the depth range of the trap experiments used. In addition, the derived equations assuming a residual free POC fraction improved POC/PIC rain ratio predictability by at most 24%, not better

than models including trap data with low mass CaCO$_3$/total mass ratios (<0.4).

[13] We also tested the possibility that the ballasted POC decays with depth, rather than sinking conservatively. In order to quantify the depth effect we compared the ratio between predicted values and measured values to depth:

$$F(z) = \{f_o.F_o(z) + f_{ca}F_{ca}(z) + f_1.F_1(z)\}/(\beta.z) \quad (6)$$

[14] Results indicate a significant relationship with depth for trap data independent of the depth interval considered for the analysis. Comparison of predicted versus measured values indicates that some of the variability in the POC/PIC rain ratios from trap experiments with high mass CaCO$_3$/total mass ratios can be explained by ballasted POC degradation at depth (Table 5) depending on trap data used. Including a depth dependent remineralization of ballasted organic carbon does not, however, improve predictions of POC fluxes and POC/PIC rain ratios when trap experiments with low mass CaCo$_3$/total mass ratios are included in the analysis (Tables 3, 4 and 5).

[15] In regions of high mass CaCO$_3$/total mass export flux, most of the variability in the POC/PIC rain ratio in the deep sea is not predictable by any version of the ballast model that we have been able to devise and is not related to differences in primary productivity (direct comparison of POC/PIC rain ratios in areas of high mass CaCO$_3$/total mass ratios with levels of primary production

Table 3. Variance Explained (in %) by the Models for POC Fluxes and POC/PIC Rain Ratios[a]

	Three Fractions		One Fraction	
	POC	POC/PIC	POC	POC/PIC
<1000 m	84	80	67	78
<2000 m	89	87	71	86
<3000 m	87	89	75	95

[a] Results are given for the model separating the mineral fractions in CaCO$_3$, opal and lithogenic material (three fractions) and the models using only the sum of mineral fractions (one fraction). Analysis was done using the selected trap experiments carried out below 1000 m depth (<1000 m), below 2000 m depth (<2000 m) and below 3000 m depth (<3000 m). All correlations coefficients between measured and predicted values are significant (P < 0.0001).

Table 4. Average POC/PIC Rain Ratios (±1 Standard Deviation) and Variance Explained (in %) by the Models for POC Fluxes and POC/PIC Rain Ratios[a]

	<1000 m	<2000 m	<3000 m
Three-Fractions Model [b]			
Percent of POC variance explained	83	88	84
Percent of POC/PIC variance explained	Ns	Ns	Ns
Average POC/PIC	0.852 ± 0.101	0.790 ± 0.114	0.765 ± 0.104
One-Fraction Model [c]			
Percent of POC variance explained	79	87	80
Percent of POC/PIC variance explained	Ns	Ns	Ns
Average POC/PIC	0.714 ± 0.110	0.653 ± 0.102	0.574 ± 0.098
Measured [d]			
Average POC/PIC	0.814 ± 0.241	0.768 ± 0.197	0.719 ± 0.215

[a] Results are given for trap experiments with mass $CaCO_3$/total mass ratios above 0.4. Models were derived from the analysis of selected trap experiments carried out below 1000 m depth (<1000 m), below 2000 m depth (<2000 m) and below 3000 m depth (<3000 m).
[b] Model based on three mineral fractions: $CaCO_3$, opal, lithogenic material (three fractions).
[c] Model based on the sum of minerals (One Fraction).
[d] Average POC/PIC rain ratios calculated from the trap data (Measured).

is significant but corresponds only to at most 6% of the variability).

[16] The importance of $CaCO_3$ in transporting carbon to the deep ocean contradicts the hypothesis based on plankton dynamics and seasonal sediment trap flux showing high opal *versus* $CaCO_3$ ratios during periods of high POC flux [*Ittekkot et al.*, 1991; *Honjo*, 1996; *Takahashi et al.*, 2000]. We, therefore, collected individual cup measurements from the traps used in the analysis of annual data (Figure 1) to investigate variability of POC fluxes as a function of composition in the mineral fraction on short timescales (4–61 days). Correlation of POC fluxes with the different mineral fractions shows similar results as for annual data (Figure 6). Again, the highest correlation coefficient is obtained for $CaCO_3$. POC versus opal fluxes show variations dependent on the mass ratio of opal/total minerals. Applying the models obtained from the analysis of annual data to the cup data gives good results (for all trap data save SP* r = 0.899 and r = 0.902, and for the reduced data set r = 0.909 and r = 0.982; for POC and POC/PIC respectively). These results confirm that the carrying coefficient as deter-

mined for the annual flux data are not an artifact of averaging but reflect mechanisms affecting POC fluxes both on an annual scale as well as on the scale relevant to biological and chemical processes.

4. Discussion

4.1. Predictability of POC Transport at Depth

[17] Multiple correlation analysis of deep-sea flux data from sediment trap experiments indicates that geographical variability in organic carbon fluxes can be accounted for, to a large extent, by the composition of associated sinking mineral particles, consistent with *Armstrong et al.* [2002]. Within a range of annual mass $CaCO_3$/total mass ratios between 0.4 and 0.8, however, estimates of average POC fluxes and the resulting POC/PIC rain ratios are similar to the measured values, but variability is poorly predicted. Measurement of particulate dissolution in trap cups could affect results as compared to the model. Few studies report values for dissolved components in the cups which may depend on sampling strategy (sampling time, preservative).
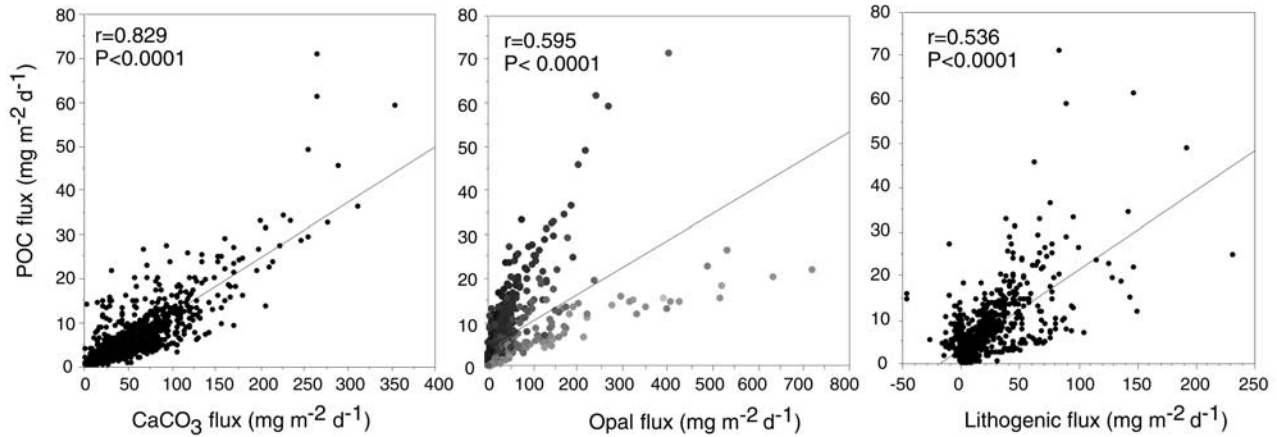
Table 5. Variance Explained (in %) by the Models for POC Fluxes and POC/PIC Rain Ratios and Average POC/PIC Rain Ratio (± 1 Standard Deviation)[a]

	<1000 m	<2000 m	<3000 m
All Trap Data			
Percent of POC variance explained	74	78	86
Percent of POC/PIC variance explained	36	72	87
$CaCO_3$ > 0.4			
Percent of POC variance explained	59	78	88
Percent of POC/PIC variance explained	12	16	33
Average predicted POC/PIC [b]	1.019 ± 0.414	0.852 ± 0.203	0.738 ± 0.114
Average measured POC/PIC [c]	0.814 ± 0.241	0.768 ± 0.197	0.719 ± 0.215

[a] Results are given for models derived using selected trap experiments below 1000 m (<1000 m), 2000 m (<2000 m) and 3000 m (<3000 m) depth and assuming that the mineral associated POC is also remineralized with depth. Results were obtained through linear regression of measured versus predicted values from trap experiments used to derive the models (all trap data) and a subset of the data with mass $CaCO_3$/total mass ratios > 0.4 ($CaCO_3$ > 0.4). All correlation coefficients between measured and predicted values are significant (P < 0.0001).
[b] Model derived average POC/PIC rain ratios for the subset of trap data with mass $CaCO_3$/total mass ratios >0.4. Values for all trap data are given in Table 4.
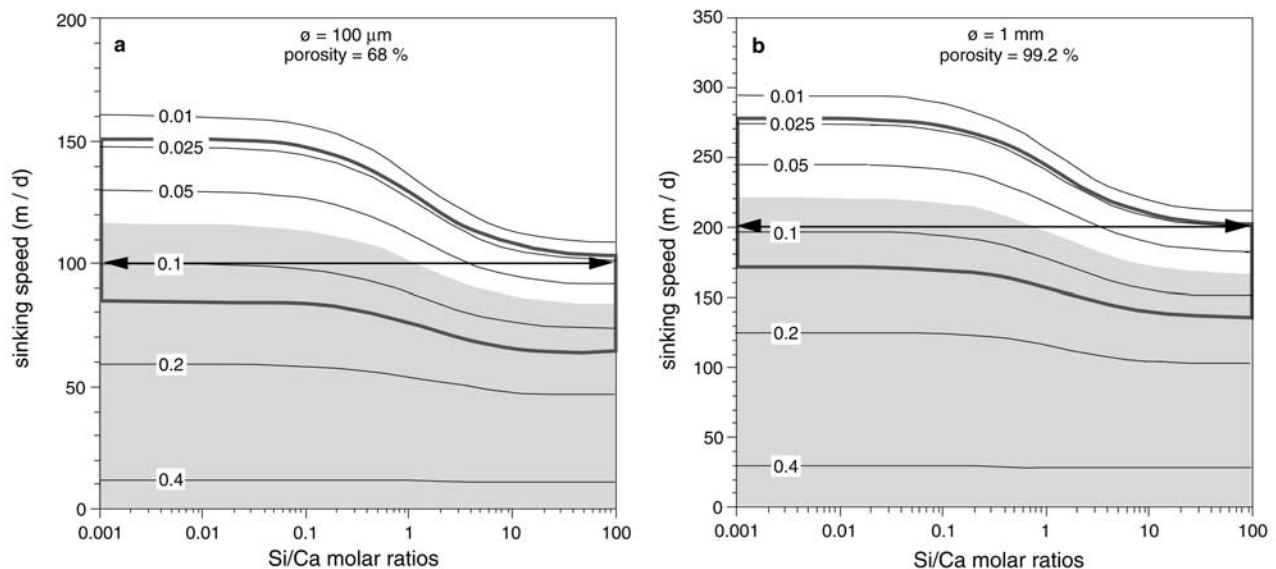[c] Average POC/PIC rain ratios calculated for the subset of trap data with mass $CaCO_3$/total mass ratios >0.4. Values for all trap data are given in Table 4.

Figure 6. Scatterplots, correlation coefficient and probability for individual cup measurements of POC flux versus $CaCO_3$, opal and lithogenic material fluxes for trap experiments below 1000 m depth. Slopes of the regression lines are 0.126 for $CaCO_3$, 0.061 for opal and 0.180 for lithogenic material. Shaded circles in the plot of POC versus opal represent the variations in mass opal/total mass ratios levels. The lighter shading corresponds to high mass opal/total mass ratios, dark shading to low mass opal/total mass ratios.

Values reported in the literature are highly variable ranging from 1.8 to over 30% for opal and 10% for POC [*von Bodungen et al.*, 1991; *Fischer and Wefer*, 1991; *Honjo and Manganini*, 1993; *Honjo et al.*, 1995]. The effect on annual estimates does not seem to exceed 10% as high dissolution tends to occur only during periods of low flux. Also, the scatterplots of POC *versus* other flux components (Figure 3) and predicted *versus* measured POC (Figure 5) do not reveal a systematic bias in trap experiments that were not corrected for dissolution effects. For several trap experiments we

Figure 7. Sinking speeds of model aggregates as a function of opal/$CaCO_3$ ratio (given as Si/Ca molar in the x axis) for mass POC/total mass ratios values of 0.4, 0.2, 0.1, 0.05, 0.025 and 0.01. The fraction of lithogenic material was assumed to be 9% of total mass, the average value in open ocean trap experiments. Sinking speeds are given for (a) a 100 μm diameter aggregate and (b) a 1 mm diameter aggregate. The horizontal double arrows indicates the mass POC/total mass ratio of particles ballasted only by $CaCO_3$ (left) or opal (right) and having same sinking speed. The shaded area corresponds to the range of sinking speeds expected from the composition (mass POC/total mass ratio) of surface trap experiments (at 200 m depth). The framed area corresponds to the range of sinking speeds expected from the composition (mass POC/total mass ratio) of deep trap experiments (below 1000 m depth).

Table 6. Predicted Benthic Fluxes Obtained From Model Run [*Archer et al.*, 2000] and Benthic POC Flux Estimates Based on Carrying Coefficients Determined in This Study and Benthic Fluxes of $CaCO_3$, SiO_2 (Opal) and Clay

	Benthic flux, 10^{12} g yr^{-1}	Predicted Org.C. carrying flux, 10^{12} g yr^{-1}	(% of total)
Org. C[a]	886		
$CaCO_3$	7438	521–617	(83–80%)
SiO_2	3255	84–95	(11–15%)
Clay	600	39–41	(5–6%)
Total		654–742	

[a] Organic carbon.

could calculate an estimate of prediction errors by propagation of analytical and splitting errors of the measurements. Error estimates for our predictions vary from ±9 to ±28% for POC fluxes and from ±10 to ±35% for POC/PIC ratios. Such estimates do not include the effects of trapping efficiency and dissolution in cups and indicate there is scope for improvement both in sediment trap methodology and reporting of results. Differences between predicted and measured values range from −59 to +129% of the measured values. Average values are ±35% for traps with annual mass $CaCO_3$/total mass ratios between 0.4 and 0.8 and ±19% for the other traps. Although our average error in estimates are close to what would be expected due to sample processing, the range observed far exceeds these values. Estimates of variability due to POC remineralization in deep trap experiments did not explain the differences between measured and predicted values. We cannot, however, totally exclude deep sea remineralization as causing at least part of the observed variability, given the relatively larger error on our predictions. Also, processes influencing remineralization at depth such as grazing and particle dynamics [*Berelson*, 2002] might be more localized and might not be resolved by an analysis on the global scale.

4.2. Theoretical Effect of Particle Composition on Sinking Speed

[18] Values for the carrying coefficients of mineral particles follow the order $CaCO_3$, lithogenic material, then opal. One potential explanation for the differences in carrying coefficient is the ballast effect. The sequence of the carrying coefficients varies in the same order as the mineral density: calcium carbonate (2.71 g cm^{-3}), lithogenic material (e.g., quartz is 2.65 g cm^{-3}), and opal (2.1 g cm^{-3}). In order to test the differential effect of mineral on density, we estimated sinking speed of aggregates as a function of composition.

[19] Sinking rates of particle 100 μm and 1 mm in diameter were calculated using the terminal velocity equation for a solid sphere at low Reynolds numbers (<0.5) and the empirical formula of *Zahm* [1927] at high Reynolds numbers [*Vogeler and Wolf-Gladrow*, 1993]. We assumed a density for organic matter of 1.06 g cm^{-3} (estimated density of a bacterial cell containing 80% water, *Logan and Hunt* [1987]). Porosity of particles was calculated using the relationship of *Alldredge and Gotschalk* [1988] between size and porosity. We used the empirical formula of *Matsumoto and Suganuma* [1977] to estimate the effect of particle

permeability on sinking rates assuming fibers diameter of 1 μm and 10 μm. Our estimates indicate that permeability increases sinking rate by 10% at most [*Masliyah and Polikar*, 1980] and should therefore not significantly affect our results. Theoretical estimates of particle sinking rates are presented as a function particle composition (ratio of opal/$CaCO_3$ presented as Si/Ca molar ratios) and mass POC/total mass ratios (Figure 7). The influence of Si/Ca on sinking rates is highest within the range found in most trap measurements (0.2 to 20). Sensitivity of sinking rates to changes in Si/Ca depends on mass POC/total mass and is not significant at values above 0.2. These calculations show that the density contrast between $CaCO_3$ and opal might be responsible for the observed factor of 2 difference in carrying coefficients. When the organic carbon fraction is 0.1 or below, variations in Si/Ca can affect the sinking velocity by up to 48% (Figure 7). This is similar to the difference in carrying capacity observed for Ca and Si when expressed in molar ratios (46%). Alternatively, at comparable sinking speeds particles containing only $CaCO_3$ as ballast carry about 2 to 4 times as much POC than particles containing only opal as ballast (double arrows in Figure 7). This is similar to the difference in carrying coefficients based on mass between $CaCO_3$ and opal.

[20] It is unclear why sinking speeds should affect POC content of particles in the deep sea: our carrying coefficients were determined from analysis of trap experiments at depths ranging from 1000 to 4833 m and did not seem to be significantly affected by depth. In addition, bacterial activities measured in the water column and in sinking organic matter below 1000 m depth tend to be very low [*Turley*, 1993; *Patching and Eardly*, 1997]. In shallow waters, where a greater fraction of sinking POC is remineralized, differences in sinking speed might influence the quantities of carbon reaching the deep sea. Within the range of mass POC/total mass ratio observed in shallower traps (0.03 to 0.43 with annual averages ranging from 0.042 to 0.24 [*Lohrenz et al.*, 1992; *Wefer and Fischer*, 1993; *Pilskaln et al.*, 1996; *Thunell*, 1998a, 1998b; *Peña et al.*, 1999; *Collier et al.*, 2000; *Conte et al.*, 2001] the ballast composition could also significantly affect sinking rates and, therefore, POC remineralization as a function of depth. As particle sinking speeds depend on a range of other parameters [*Berelson*, 2002], the effect of ballast composition on particle sinking rates and POC transport at depth is still speculative but warrants further investigation.

4.3. Implications of the Organic Carbon–Mineral Flux Association

[21] An implication of the ballast model is that changes in the sinking flux of opal [*Harrison*, 2000] or dust [*Petit et al*, 1999] might change the ratio of organic to inorganic carbon (the rain ratio). The rain affects the pCO_2 of the atmosphere by two mechanisms; by rearranging the alkalinity and total CO_2 in the water column, and by altering the global burial rate of $CaCO_3$, which in the long term drives changes in ocean pH and atmospheric pCO_2 [*Archer and Maier-Reimer*, 1994; *Archer et al.*, 2000]. *Archer and Maier-Reimer* [1994] conducted an experiment similar to the potential effect of ballast model on the rain ratio by altering

the fraction of organic carbon degradation in the water column, while maintaining everything else the same. This experiment minimizes the effect of water column chemistry rearrangement, and forces atmospheric pCO_2 entirely from the seafloor. They found that an increase in organic rain to the seafloor of 33% (from 15 to 20 μmol C cm^{-2} yr^{-1} global average) was sufficient to draw down pCO_2 by approximately 60 ppm. Their model did not include SiO_2, but a subsequent revision of the model did [*Archer et al.*, 2000]. Global benthic fluxes of organic carbon, $CaCO_3$, biogenic SiO_2, and terrigenous material from this model are given in Table 6. These were tuned to reproduce the observed benthic chemistry and global burial rates. The model organic carbon benthic flux is gratifyingly close to the predictions of the ballast model using the model benthic fluxes of $CaCO_3$, biogenic SiO_2, and terrigenous material and the carrying coefficients listed in Table 2.

[22] The telling result is that globally, 83% of the organic carbon flux to the seafloor is accounted for by $CaCO_3$ ballast. Therefore, increasing the organic carbon rain by 33% without changing $CaCO_3$ fluxes would require roughly a tripling of both opal and clay rain rates. Dust fluxes were higher during glacial time by a factor of 2–3 globally [*Rea*, 1994; *Mahowald et al.*, 1999]; by itself, this would increase organic carbon flux to the seafloor by 5–10%, significantly but not enough to explain the entire glacial/interglacial pCO_2 change.

5. Summary

[23] The model of *Armstrong et al.* [2002] proposing an association of deep sea POC fluxes with mineral ballast was tested using a global compilation of deep sediment trap experiments and distinguishing three forms of mineral ballast: calcium carbonate, opal, and lithogenic material. Our results indicate that (1) organic carbon fluxes in the deep sea can be estimated from the fluxes of calcium carbonate, opal, and lithogenic material; (2) the carrying coefficients (or mineral-associated organic carbon fractions) are similar for calcium carbonate and lithogenic material, and about 3 times higher than the carrying coefficient for opal; (3) comparison of POC fluxes estimated using our carrying coefficients and global estimates of mineral fluxes derived from model studies are similar to model estimates of POC benthic fluxes; up to 83% of global POC fluxes are associated to calcium carbonate because it is denser than opal and more abundant than terrigenous material; and (4) our results argue against large changes in the organic carbon to calcium carbonate rain ratios in the past.

References

Alldredge, A. L., and C. Gotschalk, In situ settling behavior of marine snow, *Limnol. Oceanogr.*, *33*, 339–351, 1988.

Antia, A. N., B. von Bodungen, and R. Peinert, Particle flux across the mid-European continental margin, *Deep Sea Res., Part I*, *46*, 1999–2024, 1999.

Antia, A. N., et al., Basin-wide particulate carbon flux in the Atlantic Ocean: Regional export patterns and potential for atmospheric carbon sequestration, *Global Biogeochem. Cycles*, *15*, 845–862, 2001.

Antoine, D., J.-M. André, and A. Morel, Oceanic primary production, 2, Estimation at global scale from satellite (coastal zone color scanner) chlorophyll, *Global Biogeochem. Cycles*, *10*, 57–96, 1996.

Archer, D. E., A data-driven model of the global calcite lysocline, *Global Biogeochem. Cycles*, *10*, 511–526, 1996.

Archer, D. E., and E. Maier-Reimer, Effect of deep-sea sedimentary calcite preservation on atmospheric CO_2 concentration, *Nature*, *367*, 260–264, 1994.

Archer, D. E., A. Winguth, D. Lea, and N. Mahowald, What caused the glacial/interglacial atmospheric pCO_2 cycles?, *Rev. Geophys.*, *38*, 159–189, 2000.

Armstrong, R. A., C. Lee, J. I. Hedges, S. Honjo, and S. G. Wakeham, A new, mechanistic model for organic carbon fluxes in the ocean: based on the quantitative association of POC with ballast minerals, *Deep Sea Res., Part II*, *49*, 219–236, 2002.

Behrenfeld, M. J., and P. G. Falkowski, Photosynthetic rates derived from satellite-based chlorophyll concentration, *Limnol. Oceanogr.*, *42*, 1–20, 1997.

Berelson, W. M., Particle settling rates in crease with dept in the ocean, *Deep Sea Res., Part II*, *49*, 237–251, 2002.

Catubig, N., D. E. Archer, R. Francois, P. deMenocal, and W. Howard, Global deep-sea burial rate of calcium carbonate during the Last Glacial Maximum, *Paleoceanography*, *13*, 298–310, 1998.

Collier, R., J. Dymond, S. Honjo, S. Manganini, R. François, and R. Dunbar, The vertical flux of biogenic and lithogenic material in the Ross Sea: Moored sediment trap observations 1996–1998, *Deep Sea Res., Part II*, *47*, 3491–3520, 2000.

Conte, M. H., N. Ralph, and E. H. Ross, Seasonal and interannual variability in deep ocean particle flux at the Oceanic Flux Program (OFP)/ Bermuda Atlantic Time Series (BATS) site in the western Sargasso Sea near Bermuda, *Deep Sea Res., Part II*, *48*, 1471–1505, 2001.

Deuser, W. G., E. H. Ross, and R. F. Anderson, Seasonality in the supply of sediment to the deep Sargasso Sea and implications for the rapid transfer of matter to the deep ocean, *Deep Sea Res.*, *28*, 495–505, 1981.

Dymond, J., and R. Collier, Biogenic particle fluxes in the Equatorial Pacific: Evidence for both high and low productivity during the 1982–1983 El Niño, *Global Biogeochem. Cycles*, *2*, 129–137, 1988.

Fischer, G., and G. Wefer, Sampling, preparation and analysis of marine particulate matter, *Geophys. Monogr.*, *63*, 391–397, 1991.

Fischer, G., and G. Wefer, Long-term observation of particle flux in the Eastern Atlantic: Seasonality, changes of flux with depth and comparison with the sediment record, in *The South Atlantic: Present and Past Circulation*, edited by G. Wefer et al., pp. 325–344, Springer-Verlag, New York, 1996.

François, R., S. Honjo, R. Krishfield, and S. Manganini, Factors controlling the flux of organic carbon to the bathypelagic zone of the ocean, *Global Biogeochem. Cycles*, *16*, doi:10.1029/2001GB001722, 2002.

Haake, B., V. Ittekkot, T. Rixen, V. Ramaswamy, R. R. Nair, and W. B. Curry, Seasonality and interannual variability of particle fluxes to the deep Arabian Sea, *Deep Sea Res., Part I*, *40*, 1323–1344, 1993.

Harrison, K. G., Role of increased marine silica input on paleo-pCO_2 levels, *Paleoceanography*, *15*, 292–298, 2000.

Hebbeln, D., Flux of ice-rafted detritus from sea ice in the Fram Strait, *Deep Sea Res., Part II*, *47*, 1773–1790, 2000.

Hebbeln, D., M. Marchant, and G. Wefer, Seasonal variations of the particle flux in the Peru–Chile current at 30°S under "normal" and El Niño conditions, *Deep Sea Res., Part II*, *47*, 2101–2128, 2000.

Honjo, S., Particle fluxes and modern sedimentation in the polar oceans, in *Polar Oceanography*, vol. II, edited by W. O. Smith Jr., pp. 687–739, Academic, San Diego, Calif., 1990.

Honjo, S., Fluxes of particles to the interior of the open oceans, in *Particle Flux in the Ocean*, edited by V. Ittekkot et al., pp. 91–154, John Wiley, New York, 1996.

Honjo, S., and S. J. Manganini, Annual biogenic particle fluxes to the interior of the North Atlantic Ocean; studied at 34°N 21°W and 48°N 21°W, *Deep Sea Res., Part II*, *40*, 587–607, 1993.

Honjo, S., S. J. Manganini, and G. Wefer, Annual particle flux and a winter outburst of sedimentation in the northern Norwegian Sea, *Deep Sea Res., Part I*, *35*, 1223–1234, 1988.

Honjo, S., J. Dymond, R. Collier, and S. J. Manganini, Export production of particles to the interior of the equatorial Pacific Ocean during the 1992 EqPac experiment, *Deep Sea Res., Part II*, *42*, 831–870, 1995.

Honjo, S., J. Dymond, W. Prell, and V. Ittekkot, Monsoon-controlled export fluxes to the interior of the Arabian Sea, *Deep Sea Res., Part II*, *46*, 1859–1902, 1999.

Honjo, S., R. François, S. Manganini, J. Dymond, and R. Collier, Particle fluxes to the interior of the Southern Ocean in the Western Pacific sector along 170°W, *Deep Sea Res., Part II*, *47*, 3521–3548, 2000.

Ittekkot, V., R. R. Nair, S. Honjo, V. Ramaswamy, M. Bartsch, S. Manganini, and B. N. Desai, Enhanced particle flux in Bay of Bengal induced by injections of fresh water, *Nature*, *352*, 385–387, 1991.

Jickells, T. D., P. P. Newton, P. King, R. S. Lampitt, and C. Boutle, A comparison of sediment trap records of particle fluxes from 19 to 48°N in the northeast Atlantic and their relation to surface water productivity, *Deep Sea Res., Part I*, *43*, 971–986, 1996.

Kawahata, H., M. Yamamuro, and H. Ohta, Seasonal and vertical variations of sinking particle fluxes in the West Caroline Basin, *Oceanol. Acta*, *21*, 521–532, 1998.

Kawahata, H., A. Suzuki, and H. Ohta, Export fluxes in the Western Pacific Warm Pool, *Deep Sea Res., Part I*, *47*, 2061–2091, 2000.

Kempe, S., and H. Knaack, Vertical particle flux in the Western Pacific below the North Equatorial Current and the Equatorial Counter Current, in *Particle Flux in the Ocean*, edited by V. Ittekkot et al., pp. 313–323, John Wiley, New York, 1996.

Kuss, J., and K. Kremling, Particulate trace element fluxes in the deep northeast Atlantic Ocean, *Deep Sea Res., Part I*, *46*, 149–169, 1999.

Logan, B. E., and J. R. Hunt, Advantages to microbes of growth in permeable aggregates in marine systems, *Limnol. Oceanogr.*, *32*, 1034–1048, 1987.

Lohrenz, S. E., G. A. Knauer, V. L. Asper, M. Tuel, A. F. Michaels, and A. H. Knap, Seasonal and interannual variability in primary production and particle flux in the northwestern Sargasso Sea: U.S JGOFS Bermuda Atlantic time-Series, *Deep Sea Res.*, *39*, 1373–1391, 1992.

Mahowald, N., K. E. Kohfeld, M. Hansson, Y. Balkanski, S. P. Harrison, I. C. Prentice, M. Schulz, and H. Rodhe, Dust sources and deposition during the Last Glacial Maximum and current climate: A comparison of model results with paleodata from ice cores and marine sediments, *J. Geophys. Res.*, *104*, 15,895–15,916, 1999.

Margalef, R., Life-forms of phytoplankton as survival alternatives in an unstable environment, *Oceanol. Acta*, *1*, 493–509, 1978.

Masliyah, J. B., and M. Polikar, Terminal velocity of porous spheres, *Can. J. Chem. Eng.*, *58*, 299–302, 1980.

Matsumoto, K., and A. Suganuma, Settling velocity of a permeable model floc, *Chem. Eng.*, *32*, 445–447, 1977.

Mortlock, R. A., and P. N. Froelich, A simple method for the rapid determination of biogenic opal in pelagic marine sediments, *Deep Sea Res., Part I*, *36*, 1415–1426, 1989.

Nodder, S. D., and L. C. Northcote, Episodic particulate fluxes at southern temperate mid-latitudes (42–45°S) in the Subtropical Front region, east of New Zealand, *Deep Sea Res., Part I*, *48*, 833–864, 2001.

Opdyke, B. N., and J. C. G. Walker, Return of the coral reef hypothesis: Basin to shelf partitioning of $CaCO_3$ and its effect on atmospheric pCO_2, *Geology*, *20*, 733–736, 1992.

Patching, J. W., and D. Eardly, Bacterial biomass and activity in the deep waters of the eastern Atlantic-evidence of a barophilic community, *Deep Sea Res., Part I*, *44*, 1655–1670, 1997.

Peinert, R., B. von Bodungen, and V. S. Smetacek, Food web structure and loss rate, in *Productivity of the Ocean: Present and Past*, edited by W. H. Berger, V. S. Smetacek, and G. Wefer, pp. 35–48, John Wiley, New York, 1989.

Peña, M. A., K. L. Denman, S. E. Calvert, R. E. Thomson, and J. R. Forbes, The seasonal cycle in sinking particle fluxes off Vancouver Island British Columbia, *Deep Sea Res., Part II*, *46*, 2969–2992, 1999.

Petit, J. R., et al., Climate and atmospheric history of the past 420,000 years from the Vostok ice core Antarctica, *Nature*, *399*, 429–436, 1999.

Pilskaln, C. H., J. B. Paduan, F. P. Chavez, R. Y. Anderson, and W. M. Berelson, Carbon export and regeneration in the coastal upwelling system of Monterey Bay, central California, *J. Mar. Sys.*, *54*, 1149–1178, 1996.

Ramaswamy, V., and R. R. Nair, fluxes of material in the Arabian Sea and Bay of Bengal—Sediment trap studies, *Proc. Indian Acad. Sci.*, *103*, 189–210, 1994.

Rea, D. K., The paleoclimatic record provided by eolian deposition in the deep sea: The geologic history of wind, *Rev. Geophys.*, *32*, 159–196, 1994.

Schäfer, P., V. Ittekkot, M. Bartsch, R. R. Nair, and J. Tieman, Fresh water influx and particle flux variability in the Bay of Bengal, in *Particle Flux in the Ocean*, edited by V. Ittekkot, P. Schäfer, S. Honjo, and P. J. Depetris, pp. 313–323, John Wiley, New York, 1996.

Smetacek, V. S., R. Scharek, and E.-M. Nöthig, Seasonal and regional variation in the pelagial and its relationship to the life history cycle of krill, in *Antarctic Ecosystems*, edited by K. R. Kerry and G. Hempel, pp. 103–114, Springer-Verlag, New York, 1990.

Suess, E., and C. A. Ungerer, Element and phase composition of particulate matter from the circumpolar current between New Zealand and Antarctica, *Oceanol. Acta*, *4*, 151–160, 1981.

Takahashi, K., N. Fujitani, M. Yanada, and Y. Maita, Long-term biogenic particle fluxes in the Bering Sea and the central subarctic Pacific Ocean 1990–1995, *Deep Sea Res., Part I*, *47*, 1723–1759, 2000.

Thunell, R. C., Particle fluxes in a coastal upwelling zone: Sediment trap results from Santa Barbara Basin California, *Deep Sea Res., Part II*, *45*, 1863–1884, 1998a.

Thunell, R. C., Seasonal and annual variability in particle fluxes in the Gulf of California: a response to climate forcing, *Deep Sea Res., Part I*, *45*, 2059–2083, 1998b.

Thunell, R. C., C. H. Pilskaln, E. Tappa, and L. R. Sautter, Temporal variability in sediment fluxes in the San Pedro Basin Southern California Bight, *Cont. Shelf Res.*, *14*, 333–352, 1994.

Tsunogai, S., and S. Noriki, Organic matter fluxes and the sites of oxygen consumption in deep water, *Deep Sea Res., Part I*, *34*, 755–767, 1987.

Turley, C. M., The effect of pressure on leucine and thymidine incorporation by free-living bacteria and by bacteria attached to sinking oceanic particles, *Deep Sea Res., Part I*, *40*, 2193–2206, 1993.

Tyrell, T., and A. H. Taylor, A modeling study of Emiliania huxleyi in the NE Atlantic, *J. Mar Syst.*, *9*, 83–112, 1996.

von Bodungen, B., M. Wunsch, and H. Fürderer, Sampling and analysis of suspended and sinking particles in the northern north Atlantic, *Geophys. Monogr.*, *63*, 1991.

Vogeler, A., and D. A. WolfGladrow, Pair interaction lattice gas simulations: Flow past obstacles in two and three dimensions, *J. Stat. Phys.*, *71*, 163–190, 1993.

Wefer, G., and G. Fischer, Seasonal patterns of vertical particle flux in equatorial and coastal upwelling areas of the eastern Atlantic, *Deep Sea Res., Part I*, *40*, 1613–1645, 1993.

Wefer, G., G. Fischer, D. K. Futterer, R. Gersonde, S. Honjo, and D. Ostermann, Particle sedimentation and productivity in Antarctic waters of the Atlantic sector, in *Geological History of the Polar Oceans: Arctic Versus Antarctic*, edited by U. Bleil and J. Thiede, pp. 363–379, Kluwer Acad., Norwell, Mass., 1990.

Wollast, R., and L. Chou, Distribution and fluxes of calcium carbonate along the continental margin in the Gulf of Biscay, *Aquatic Geochem.*, *4*, 369–393, 1998.

Wong, C. S., F. A. Whitney, D. W. Crawford, K. Iseki, R. J. Matera, W. K. Johnson, J. S. Page, and D. Timothy, Seasonal and interannual variability in particle fluxes of carbon, nitrogen and silicon from time series of sediment traps at Ocean Station P, 1982–1993: Relationship to changes in subarctic primary productivity, *Deep Sea Res., Part II*, *46*, 2735–2760, 1999.

Zahm, A. F., Flow and drag formulas for simple quadrics, *Tech. Rep. 253*, Natl. Adv. Comm. for Aeronaut., NASA Goddard Space Flight Center, Greenbelt, Md., 1927.

————————————

D. E. Archer, Department of the Geophysical Sciences, University of Chicago, 5734 S. Ellis Avenue, Chicago, IL 60637, USA. (archer@geosci.uchicago.edu)

C. Klaas, Max-Planck-Institute for Biogeochemistry, Winzerlaer 10, 07745 Jena, Germany. (cklaas@bgc-jena.mpg.de)